1998

Molecular Characterization of the α-Glucosidase Gene (*malA*) from the Hyperthermophilic Archaeon *Sulfolobus solfataricus*

Michael Rolfsmeier
University of Nebraska-Lincoln

Cynthia Haseltine
University of Nebraska-Lincoln

Elisabetta Bini
University of Nebraska-Lincoln

Amy Clark
University of Nebraska-Lincoln

Paul H. Blum
University of Nebraska - Lincoln, pblum1@unl.edu

JOURNAL OF BACTERIOLOGY, Mar. 1998, p. 1287–1295 Vol. 180, No. 5
0021-9193/98/$04.00+0

Molecular Characterization of the α-Glucosidase Gene (*malA*) from the Hyperthermophilic Archaeon *Sulfolobus solfataricus*

MICHAEL ROLFSMEIER, CYNTHIA HASELTINE, ELISABETTA BINI, AMY CLARK, AND PAUL BLUM*

George Beadle Center for Genetics, School of Biological Sciences, University of Nebraska, Lincoln, Nebraska 68588-0666

Received 18 September 1997/Accepted 12 December 1997

Acidic hot springs are colonized by a diversity of hyperthermophilic organisms requiring extremes of temperature and pH for growth. To clarify how carbohydrates are consumed in such locations, the structural gene (*malA*) encoding the major soluble α-glucosidase (maltase) and flanking sequences from *Sulfolobus solfataricus* were cloned and characterized. This is the first report of an α-glucosidase gene from the archaeal domain. *malA* is 2,083 bp and encodes a protein of 693 amino acids with a calculated mass of 80.5 kDa. It is flanked on the 5′ side by an unusual 1-kb intergenic region. Northern blot analysis of the *malA* region identified transcripts for *malA* and an upstream open reading frame located 5′ to the 1-kb intergenic region. The *malA* transcription start site was located by primer extension analysis to a guanine residue 8 bp 5′ of the *malA* start codon. Gel mobility shift analysis of the *malA* promoter region suggests that sequences 3′ to position −33, including a consensus archaeal TATA box, play an essential role in *malA* expression. *malA* homologs were detected by Southern blot analysis in other *S. solfataricus* strains and in *Sulfolobus shibatae*, while no homologs were evident in *Sulfolobus acidocaldarius*, lending further support to the proposed revision of the genus *Sulfolobus*. Phylogenetic analyses indicate that the closest *S. solfataricus* α-glucosidase homologs are of mammalian origin. Characterization of the recombinant enzyme purified from *Escherichia coli* revealed differences from the natural enzyme in thermostability and electrophoretic behavior. Glycogen is a substrate for the recombinant enzyme. Unlike maltose hydrolysis, glycogen hydrolysis is optimal at the intracellular pH of the organism. These results indicate a unique role for the *S. solfataricus* α-glucosidase in carbohydrate metabolism.

Microbes which are native to boiling acid hot springs include five genera assigned by 16S rRNA sequencing, G+C mole percent composition, metabolic characteristics, and protein sequence conservation studies to the order *Sulfolobales* (8). The order *Sulfolobales* is placed within the crenarchaeotal subdivision of the archaea (49). *Sulfolobus* is the largest genus in this order, comprising at least six species. These include *S. acidocaldarius* (5), *S. solfataricus* (13), *S. shibatae* (15, 52), *S. metallicus* (23), *S. icelandicus* (54), and *S. hakonensis* (44), all of which are obligate aerobes and either facultative chemoheterotrophs or strict lithoautotrophs. Most physiological and biochemical studies, however, focus on only three species, *S. solfataricus*, *S. acidocaldarius*, and *S. shibatae.*

S. solfataricus exhibits diverse modes of metabolism in batch culture at temperatures ranging between 70 and 90°C. It grows lithoautotrophically by oxidizing sulfur (5, 25, 50) and chemoheterotrophically on reduced-carbon compounds (13, 16, 19). Despite this metabolic flexibility, the utilization of reduced-carbon nutrients such as plant-derived starch or cellulose is poorly understood. Input of such carbon is typically rare in acidic hot springs and depends upon external factors such as fire or wind. Since polysaccharide hydrolysis and sugar carmelization are active processes in hot acid environments, successful competition for carbohydrates should necessitate mechanisms for rapid assimilation. Endogenous reserves of starch in plants and exogenous starch utilization in microbes often depend upon an α-amylase which generates linear maltodextrins as well as an α-glucosidase (maltase) which converts maltose and maltodextrins to glucose (26). In animals, however, α-glucosidases are also critical for utilization of intracellular stores of glycogen. For example, glycogen storage disease (Pompe's disease) in humans is a direct consequence of α-glucosidase deficiency (21). Many α-glucosidase genes from eukaryotic and eubacterial organisms have been cloned and characterized (20). Although such enzymes also occur among the archaea (10, 40), none of their corresponding genes have yet been characterized, precluding an analysis of their intracellular functions or evolutionary origins.

Members of the genus *Sulfolobus* utilize starch as the sole carbon and energy source (16) and have both α-amylase and α-glucosidase activities (4). It has been reported, however, in surveys of *Sulfolobus* species that carbohydrate utilization profiles are distinct (16). For example, *S. solfataricus* contains a β-glycosidase (17, 34) which appears to be largely absent in *S. acidocaldarius* (17). We recently reported the purification and characterization of the major soluble α-glucosidase (maltase) and the secreted α-amylase from *S. solfataricus* (19, 40). To further explore archaeal mechanisms for carbohydrate utilization and to examine their relationship with those of eukaryotes and eubacteria, the α-glucosidase gene from *S. solfataricus* was cloned and characterized, and its distribution and associated activity in common *Sulfolobus* cultivars were examined.

MATERIALS AND METHODS

Strains and cultivation. The identity of *S. solfataricus* 98/2 (22, 40) was confirmed by DNA sequence analysis of a cloned PCR fragment spanning residues 99 to 626 of the 16S rRNA gene. The GenBank accession numbers for this sequence and that determined for *S. solfataricus* P2 (DSM 1617) are L36990 and L36991, respectively. Comparison of the resulting sequences with previously published citations for *S. shibatae* (GenBank accession no. M32504) and *S. acidocaldarius* (30, 35, 53) (GenBank accession no. X03235) confirmed the identity

* Corresponding author. Mailing address: School of Biological Sciences, E234, Beadle Center for Genetics, University of Nebraska, Lincoln, NE 68588-0666. Phone: (402) 472-2769. Fax: (402) 472-8722. E-mail: pblum@crcvms.unl.edu.

of strain 98/2 as *S. solfataricus*. Cells were cultured at 80°C in a minimal salts medium (1), modified as described previously (5), at pH 3.0 with various carbohydrates at 0.2% (wt/vol) as sole carbon and energy sources. All manipulations of *Escherichia coli* were as described previously (38).

Molecular biology methods. Restriction digestion and ligation of DNA were performed as described previously (3). Plasmid transformation was performed with DH5α cells as described previously (18). Isolation of plasmid DNA was performed by the alkali lysis procedure (2). DNA sequence analysis was as described previously (39), and DNA alignment and analysis were performed with the fragment assembly programs of the Wisconsin Genetics Computer Group software package, version 8.1.

Southern blot analysis was performed essentially as described previously (41). Genomic DNA was isolated from *S. solfataricus* 98/2 as described previously (52). Fractionated genomic DNA restriction digests were transferred electrophoretically to Nytran extra-strength membranes (Schleicher and Schuell) or Hybond N membranes (Amersham) overnight in 25 mM sodium phosphate buffer (pH 6.4) at 250 mA in a water-cooled chamber. Blots were probed under stringent conditions at 42°C with 50% (vol/vol) formamide, 5× SSPE (1× SSPE is 0.15 M NaCl, 10 mM NaH_2PO_4, and 1 mM EDTA [pH 7.7]), 5× Denhardt's reagent, 0.5% (wt/vol) sodium dodecyl sulfate (SDS), and 200 ng of yeast tRNA per ml as described previously (41). The *malA* probe used for Southern blot analysis was radiolabeled by using random hexanucleotide primers and Klenow enzyme as described by the manufacturer (Boehringer Mannheim). PCR was performed with *Taq* DNA polymerase (Boehringer Mannheim) under the conditions suggested by the manufacturer.

The *S. solfataricus* library was prepared by using genomic DNA partially digested with *Sau*3AI, which was then fractionated on a 30% sucrose gradient, and DNA in a size range of 9 to 23 kb was cloned into the *Bam*HI site of phage λGEM11 (Promega). Ligation reaction products were packaged with the Pack-A-Gene extract (Promega) and used to infect *E. coli* NM539 according to the manufacturer's protocol. Individual phage plaques were then picked and propagated. Lysates were stored at −80°C with 7% (vol/vol) dimethyl sulfoxide. Library screening was performed by application of the individual lysates as a series of dot blots on nitrocellulose membranes followed by Southern blot analysis.

Recovery of a *malA* PCR product. The α-glucosidase was purified, denatured, and resolved by SDS-polyacrylamide gel electrophoresis (SDS-PAGE) as described previously (40). Protein was transferred electrophoretically to Problot membranes (Applied Biosystems), and the mature N-terminal protein sequence was determined by gas phase sequencing. Determination of internal sequence composition was accomplished by chemical cleavage of the purified protein with cyanogen bromide as described previously (32). The resulting peptides were fractionated by SDS-PAGE, transferred to membranes, and sequenced as for the mature protein. The resulting sequence information was used to design degenerate oligonucleotides, using inosine to reduce primer degeneracy. The oligonucleotides used were 5′-AA(A/G)AT(T/A/C)TA(T/C)GA(A/G)AA(T/C)AG(A/G)GG-3′ as the upper primer and 5′-GC(G/A)TAIA(A/G)IA(A/G)(G/A)TA(C/T)TTICC-3′ as the lower primer, where parentheses indicate additional nucleotides at positions of degeneracy. The resulting PCR product was blunted with Klenow enzyme and ligated to pACYC184 at the *Eco*RV site.

Northern blot analysis. *S. solfataricus* total RNA was extracted as described previously (9) from 100-mg amounts of wet cell paste derived from mid-exponential-phase maltose-grown cells. Nuclease activity was minimized by harvesting and processing cells within 2 min. Electrophoresis of RNA samples was as described previously (6), and the RNA was then electrophoretically transferred to Nytran extra-strength or Hybond N membranes and cross-linked by UV irradiation. Two types of probes were used for Northern blot analysis: double-stranded DNA (dsDNA) probes were generated as described for Southern blot analysis, and RNA probes (riboprobes) were generated by using the riboprobe buffer kit (Promega) and the manufacturer's protocol. The riboprobe template was the *malA* region comprising bp 141 to 2265 cloned into plasmid pT7T3 18U (Pharmacia). Northern hybridizations with riboprobes were performed at 55°C with 50% formamide. Northern hybridizations with DNA probes were performed as described for Southern hybridizations. Washed membranes were used to prepare autoradiograms with Kodak X-Omat film. Molecular weight standards were RNA transcripts (United States Biochemicals).

Primer extension analysis. Primer extension was performed essentially as described previously (46). The extension primer was 5′-ATGGTTCTCCTATA ACTACTTTGTAAACGC-3′ and was end labeled by using phage T4 polynucleotide kinase (New England Biolabs). The labeled oligonucleotide was purified by C_{18} chromatography as described previously (41). Total RNA for primer extension analysis was prepared as described for Northern blot analysis. Forty micrograms of RNA was hybridized to 100,000 cpm of labeled primer for 90 min at 65°C. The resulting products were analyzed on 6% (wt/vol) Long Ranger (FMC Bioproducts) acrylamide gels containing 7 M urea, using DNA sequencing reaction products as size standards. Gels were then dried and used to prepare autoradiograms.

Heterologous expression. A 2.1-kb region spanning bp 141 to 2265, encompassing the *malA* coding region and 30 bp of flanking sequence, was blunted and cloned into the *Sma*I site of pUC19. This construct was then digested with *Kpn*I and *Pst*I, and the resulting 2.1-kb fragment was subcloned into the *Kpn*I and *Pst*I sites of plasmid pLITMUS 29 (New England Biolabs). The pLTIMUS 29 derivative was then digested with *Stu*I and *Pvu*II and religated to itself to remove a T7 promoter located 3′ to the *malA* sequence. The resulting plasmid was introduced into *E. coli* DH5α for production of the recombinant protein by using stationary-phase cell suspensions, typically in 0.5 liter amounts. Cells were recovered by centrifugation and resuspended in 100 mM sodium acetate (pH 4.5) to a final density of 4×10^{10} cells/ml. Cells were broken by sonication as described previously (29). Assays for α-glucosidase activity with *p*-nitrophenyl-α-D-glucopyranoside were performed as described previously (40). In enzymatic assays for hydrolysis of maltose and glycogen, release of glucose was monitored with a glucose oxidase assay kit (Sigma) as described previously (40). *E. coli* DH5α containing pLITMUS 29 without the *malA* insert was processed and assayed in an identical manner for use as a negative control in the assays. All assays were performed in duplicate, and the results were averaged. Proteins were resolved by SDS-PAGE under reducing conditions with unstained low- and high-molecular-weight markers (Bio-Rad). Prior to electrophoresis, samples were adjusted to 2% (wt/vol) SDS and 3 mM β-mercaptoethanol and boiled for 10 min. Complete denaturation of the maltase required pretreatment with 6 M guanidine hydrochloride as described previously (40). SDS-polyacrylamide gels were stained with Coomassie blue R250 to visualize protein.

Phylogenetic analysis. Phylogenetic analyses (distance and parsimony) were performed with PHYLIP 3.57c (14). Maximum-likelihood analysis utilized the program PUZZLE (43). A multiple-sequence alignment was made by using the program CLUSTAL W (45). SEQBOOT was used to generate 100 bootstrapped data sets. Distance matrices were calculated with PROTDIST with the Dayhoff PAM matrix option. One hundred unrooted trees were inferred by neighbor-joining analysis of the distance matrix data by using NEIGHBOR. Bias introduced by the order of sequence addition was minimized by randomizing the input order. The most frequent branching order was determined with CONSENSE. The most parsimonious tree was determined with PROTPARS and CONSENSE for analysis of the SEQBOOT bootstrapped data sets.

Gel mobility shift analysis. Gel mobility shift assays were performed generally as described previously (7). The labeled probe was generated by the incorporation of [α-^{32}P]dATP into the 5′ overhanging end of a purified restriction fragment. Cell extracts used as a source of DNA binding proteins were prepared as described previously (24). Briefly, mid-exponential-phase cultures of *S. solfataricus* 98/2 were harvested by centrifugation, resuspended, and lysed by addition of Triton X-100. The resulting lysate was clarified by centrifugation, glycerol was added to a final concentration of 20% (vol/vol), and the extract was rapidly frozen and stored at −80°C. Labeled probe with or without added unlabeled competitor DNAs was incubated with cell extract at 70°C for 30 min, and the samples were then analyzed by nondenaturing PAGE. The resulting gel was dried and used to prepare autoradiograms.

Nucleotide sequence accession number. The sequence resulting from analysis of regions lying 3′ to the *malA* coding region has been deposited in GenBank under accession no. AF042494.

TABLE 1. Generation times and α-glucosidase activities of *Sulfolobus* species during growth on different sole carbon and energy sources

Organism	Generation time (h) on:			Sp act[a] (μmol of *p*-nitrophenol/min/mg) on:		
	Glucose	Maltose	Starch	Glucose	Maltose	Starch
S. solfataricus 98/2	8	8	10	130 ± 3	221 ± 9	230 ± 26
S. shibatae	12	9	14	29 ± 2	181 ± 21	228 ± 35
S. acidocaldarius	23	NG[b]	12	<0.1	ND[c]	12 ± 2

[a] Variations between replicate samples are indicated.
[b] NG, no growth.
[c] ND, not determined.

RESULTS

Generation times and α-glucosidase activities of *Sulfolobus* species on sole carbon sources. To better understand the metabolic relatedness between several of the better-characterized *Sulfolobus* species, the ability to utilize starch and its degradation products, maltose and glucose, as sole carbon and energy sources was evaluated in batch culture (Table 1). Both *S. solfataricus* 98/2 and *S. shibatae* utilized all three carbon sources with various efficiencies, as indicated by their respective generation times. *S. acidocaldarius*, however, exhibited a more limited carbon source utilization pattern. No growth was evident for *S. acidocaldarius* on maltose; however, contrary to previous reports (16, 27) growth was observed on glucose.

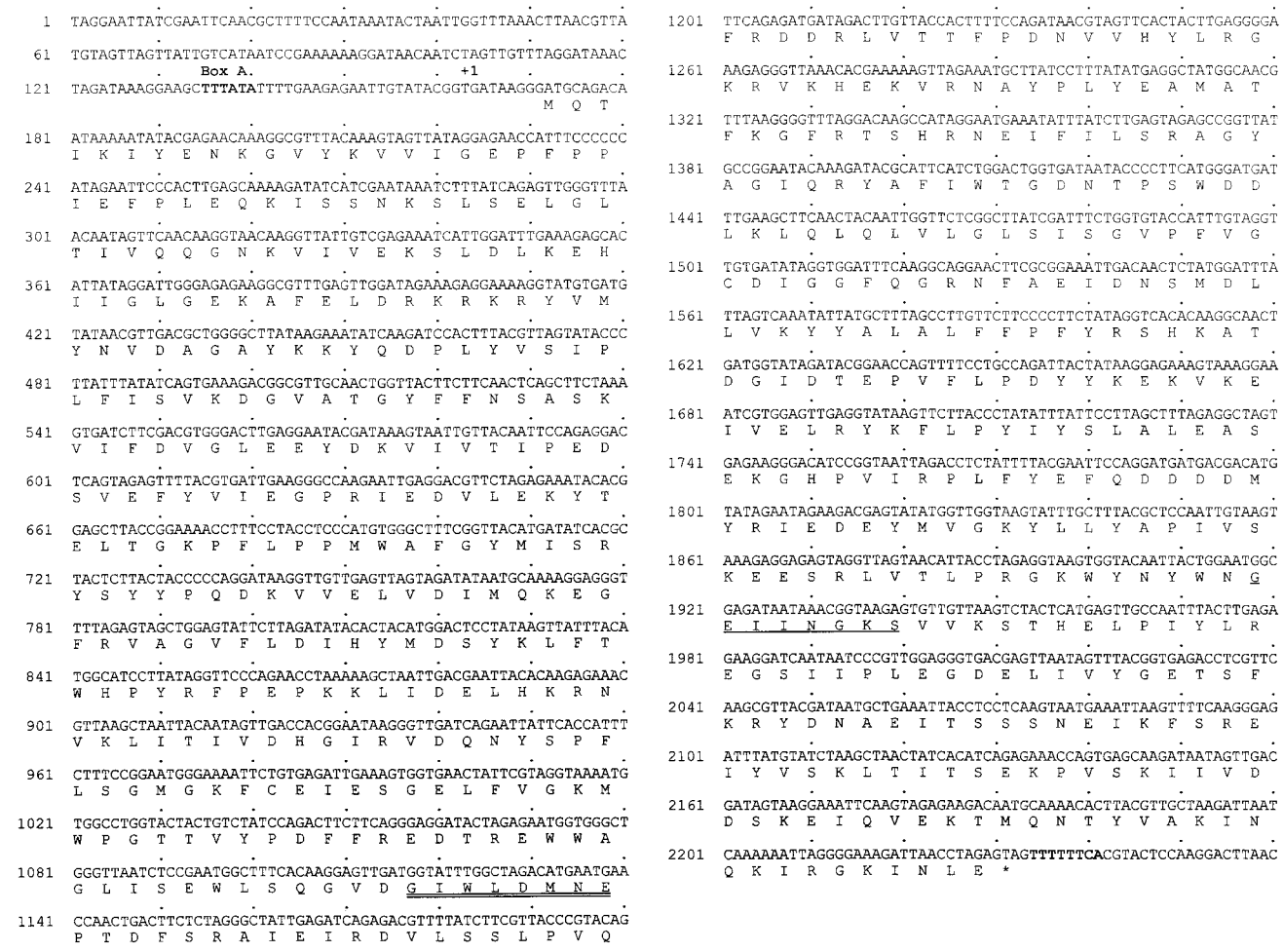

FIG. 1. DNA sequence analysis of *malA*. Glycosyl hydrolase and ATP/GTP binding motifs are indicated by double and single underlining, respectively. Putative promoter and termination sequences are in boldface. The start of transcription is indicated as +1.

α-Glucosidase activities in crude cell extracts of *S. solfataricus* and *S. shibatae* were typically 10-fold greater than those seen with *S. acidocaldarius* during growth on all carbon sources (Table 1). Activities varied nearly twofold for *S. solfataricus* (comparing all carbon sources), while in *S. shibatae*, α-glucosidase activity was six- to sevenfold higher during growth on maltose or starch than during growth on glucose. α-Glucosidase in *S. acidocaldarius* was undetectable during growth on glucose and was 28-fold lower during growth on starch relative to that of either of the other two species.

Cloning and characterization of the *S. solfataricus malA* gene. To further investigate the apparent differences in polysaccharide utilization of maltose by these *Sulfolobus* species, the gene encoding the α-glucosidase from *S. solfataricus* was cloned and characterized. Cloning of the gene was accomplished by using gene-specific PCR primers derived from the *S. solfataricus* α-glucosidase protein sequence. Amino acid sequencing indicated that the mature N-terminal maltase sequence was MQTIKIYENLGVYLWIGEP. Since the purified *S. solfataricus* α-glucosidase is generally resistant to proteolytic degradation (40), protein fragments for internal N-terminal sequence analysis were generated by chemical cleavage with cyanogen bromide. A fragment of 19 kDa was selected and yielded the N-terminal sequence VGKYLLYAPI. The resulting amino acid sequence information was used to design degenerate oligonucleotides which were then used to amplify a DNA fragment of 1.6 kb by PCR. A 731-bp *Hin*dIII-*Eco*RV fragment derived from the resulting 1.6-kb PCR product was used to generate a radiolabeled probe for Southern hybridization to verify the origin of the amplification product. This probe cross-hybridized with single DNA fragments of 1.2, 1.7, and 1.4 kb in *Hin*dIII, *Xba*I, and *Hin*cII genomic digests, respectively, of *S. solfataricus* DNA. The probe was used to screen a genomic *S. solfataricus* phage λ library consisting of 672 individually propagated recombinant phages by Southern blot analysis. A single isolate was identified (λ-7F7), which contained a 15.1-kb insert of *S. solfataricus* DNA. Southern blot analysis of restriction digests of the λ-7F7 phage was performed with the PCR-derived probe. Cross-hybridizing restriction fragments which were identical in size to those observed previously with genomic DNA were observed and indicated that the α-glucosidase-coding region is contained in a 4.3-kb *Bam*HI fragment of the λ-7F7 insert. This 4.3-kb *Bam*HI fragment was subcloned and sequenced. The sequence located immediately 5′ to the *malA* coding region was subcloned from λ-7F7 as a 2.3-kb *Sac*I-*Hin*dIII fragment. A 344-bp *Sac*I-*Bam*HI fragment from the extreme 5′ end of this fragment was used as a Southern blot probe to identify the next upstream overlapping λ clone from the genomic *S. solfataricus* 98/2 library. This isolate was named λ-1H4. A 4.1-kb *Hin*dIII-*Sac*I

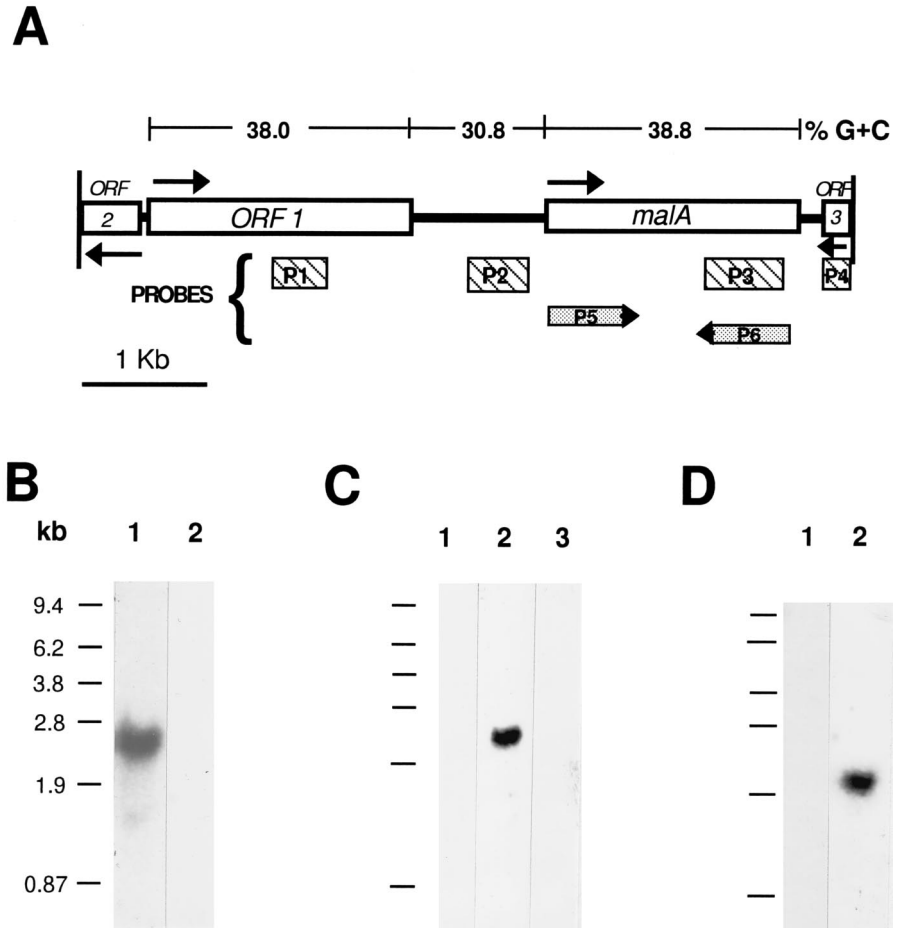

FIG. 2. Northern blot analysis of the *malA* region. (A) Schematic diagram of the *malA* region. Numbers indicate G+C mole percent compositions. (B, C, and D) Northern blots of the *malA* region. (B) Lane 1, probe P1; lane 2, probe P2. (C) Lane 1, probe P2; lane 2, probe P3; lane 3, probe P4. (D) Riboprobes. Lane 1, probe P5; lane 2, probe P6.

fragment which cross-hybridized to the same *Sac*I-*Bam*HI 344-bp fragment was subcloned from λ-1H4. A 2-kb segment of this 4.1-kb *Hin*dIII-*Sac*I fragment was sequenced to complete the analysis of putative genes lying 5′ to *malA*. Analysis of regions lying 3′ to the *malA* coding region was done with a 1.8-kb 3′ overlapping *Hin*dIII-*Hin*dIII fragment derived from λ-7F7. The resulting sequence, comprising a nearly 7-kb DNA contig, has been deposited in GenBank (see Materials and Methods).

The α-glucosidase open reading frame (ORF) (*malA*) was identified by comparison of peptide sequences derived from the N-terminal and internal N-terminal sequencing of the natural protein to the deduced amino acid sequence (Fig. 1). The *malA* sequence comprises 2,083 bp encoding a protein of 693 amino acids with a predicted mass of 80.5 kDa. This closely corresponds to the apparent mass of the previously purified enzyme subunit (40). Sequence analysis of the deduced *malA* product identified a glycosyl hydrolase motif at residues 316 to 323 and an ATP/GTP binding site motif (P loop) at residues 583 to 590 (single underline). The glycosyl hydrolase motif contains the putative active-site asparagine previously identified for the human α-glucosidase gene (20). Only two cysteine residues are evident, consistent with the low cysteine content seen previously in thermophilic proteins. There are 14 methionine residues, and the predicted mass of the largest sequence uninterrupted by methionines is 19 kDa, as suggested by the cyanogen bromide cleavage pattern of the α-glucosidase. The codon composition favors adenosine or thymidine in the wobble position, as expected for the 38 mol% G+C *malA* coding sequence. Significant bias was evident for arginine; this amino acid is coded for twice by CG(A/T/C/G) codons and 31 times by AG(G/A) codons. However, contrary to the apparent low G+C content of the genome of this organism, four amino acids (asparagine, tyrosine, phenylalanine, and histidine) which can be coded for by codons with either a C or a T in the third position show no bias towards T. Additional examination of the 7.05-kb contig identified several ORFs (Fig. 2A) with G+C contents of 37 to 38 mol%, as expected from previous analysis (13, 15). No sequence homologs of these ORFs were evident in searches of sequence databases. An unusual intergenic region of nearly 1 kb located immediately 5′ to *malA* was identified in this contig. It exhibits a G+C content of 30.8 mol%, a value considerably lower than that for the flanking coding regions.

Northern blot analysis of the *malA* region. Northern blot analysis was performed to evaluate the expression of *malA* and its surrounding regions during growth of *S. solfataricus* on maltose as the sole carbon and energy source. Probes P1 to P4 were dsDNA probes, and probes P5 and P6 were RNA probes (riboprobes). A probe derived from a 682-bp *Cla*I-*Hin*cII fragment from the 3′ end of the *malA* coding region (Fig. 2A, probe P3) cross-hybridized to a single transcript of approximately 2.4 kb, indicating that *malA* is expressed during growth

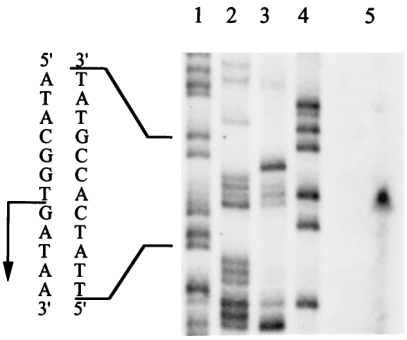

FIG. 3. Primer extension analysis of *malA*. Lanes 1 to 4, DNA sequencing reactions (T, C, G, and A, respectively); lane 5, primer extension product.

on maltose (Fig. 2C, lane 2). Probes derived from regions either 5′ or 3′ to the *malA* coding region were used to assess gene expression of immediately flanking sequences. These included an *Eco*RV-*Eco*RI fragment of 499 bp located 150 bp 5′ to *malA* (Fig. 2A, probe P2) and an *Eco*RI-*Bam*HI fragment of 231 bp located 192 bp 3′ to *malA* (Fig. 2A, probe P4). No cross-hybridization was evident with either of these probes (Fig. 2C, lanes 1 and 3). An additional probe (Fig. 2A, probe P1) was used to examine expression of ORF1, located approximately 1 kb 5′ of *malA*. This probe was derived from a *Sac*I-*Bam*HI fragment located in the center of ORF1. An approximately 2.4-kb transcript was detected with this probe (Fig. 2B, lane 1), while again no transcript was evident with probe P2 (Fig. 2B, lane 2). Riboprobes (Fig. 2A, probes P5 and P6) were used to determine the direction of transcription of *malA*. The 2.4-kb transcript was evident with the antisense riboprobe P6 (Fig. 2D, lane 2), while no transcript was detected with the sense riboprobe P5 (Fig. 2D, lane 1). These results indicate that the *malA* gene is transcribed from a site immediately adjacent to the gene and away from the large noncoding intergenic region.

Characterization of the *malA* regulatory region. There is a potential archaeal promoter sequence located 32 bp 5′ to the start codon of the *malA* gene (Fig. 1). The putative promoter (TTTATA) closely matches the consensus promoter sequence for *Sulfolobus* (37). A box B motif (TGA) (37) is also evident 7 bp 5′ to the *malA* start codon. Primer extension analysis indicated that *malA* transcription initiates on the guanine of the putative box B motif (Fig. 3). The mapped start site is 8 bp 5′ to the *malA* start codon. Although there is a potential ribosome binding site spanning positions −3 to +3, which are complementary to the six 3′-terminal bases of the 16S rRNA of *S. solfataricus* (30, 35, 53), this sequence overlaps in part the site of *malA* transcription initiation. The utilization of this sequence for the initiation of translation is therefore unclear. The *malA* mRNA is only slightly larger than the coding region of the gene (Fig. 2). Since transcription initiates very close to the start of the coding region, termination of transcription of the gene must occur close to the end of *malA*. The near-consensus terminator sequence (TTTTTCA) (11) located immediately 3′ to the stop codon of *malA* may play a role in this process.

The interaction between purified archaeal TATA binding proteins and archaeal promoters can be characterized by gel shift analysis (36). Crude cell extracts prepared as described previously for use in an in vitro transcription system (24) were used as sources of DNA binding proteins. The probe was a 233-bp *Eco*RI fragment which starts 151 bp 5′ to the *malA* transcription start site and extends 80 bp into the *malA* transcript (Fig. 4, lane 1 and *malA* p-L). Addition of crude cell extract resulted in the formation of two retarded protein DNA complexes (A and B) (Fig. 4, lane 2). Both complexes were eliminated by addition of the 233-bp *Eco*RI *malA* promoter fragment as an unlabeled competitor DNA (Fig. 4, lane 3). The more rapidly migrating complex (Fig. 4, complex B) was lost in response to addition of competitor DNA consisting of a 231-bp *Eco*RI-*Pvu*II fragment from plasmid pUC19, indicating that it was the result of nonspecific interactions. Addition of a competitor DNA comprised of a deletion derivative of the *malA* *Eco*RI promoter fragment, lacking sequences from bp −33 to +81, including the TATA box (Fig. 4, *malA* p-S), again eliminated only the lower band (Fig. 4, lane 5). These results suggest that sequences located between bp −33 and +81 are important features of the *malA* promoter.

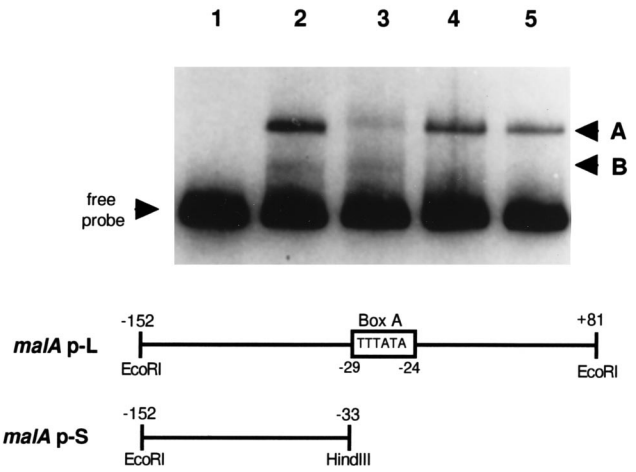

FIG. 4. Gel shift analysis of the *malA* promoter region. Lane 1, probe (*malA* p-L); lane 2, probe and 5 μg of cell extract; lane 3, probe, extract, and unlabeled probe; lane 4, probe, extract, and unlabeled competitor (*malA* p-S); lane 5, probe, extract, and unlabeled pUC19 DNA. A and B indicate the positions of retarded complexes. At the bottom schematic diagrams of *malA* fragments used as probe and competitor are shown.

***malA* distribution among *Sulfolobus* species.** Southern blot analysis with a *malA* gene probe was performed to analyze the distribution of this gene among the three commonly cultivated *Sulfolobus* species. Two isolates of *S. solfataricus* were included

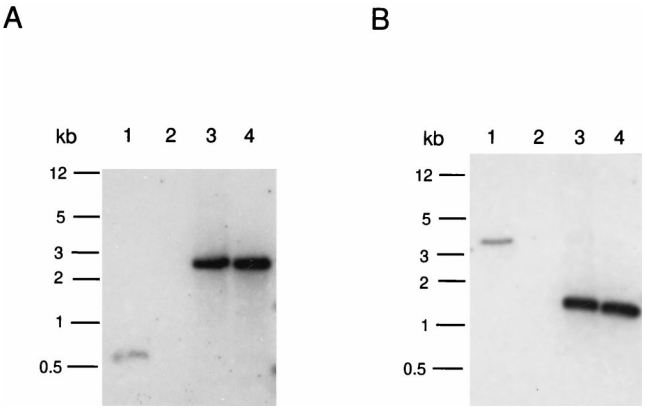

FIG. 5. Distribution of *malA* determined by Southern blot analysis. The probe comprised bp 714 to 1445 of *malA*. (A) *Eco*RV digests. (B) *Hin*dIII digests. Lanes: 1, *S. shibatae* DNA; 2, *S. acidocaldarius* DNA; 3, *S. solfataricus* 98/2 DNA; 4, *S. solfataricus* P2 DNA.

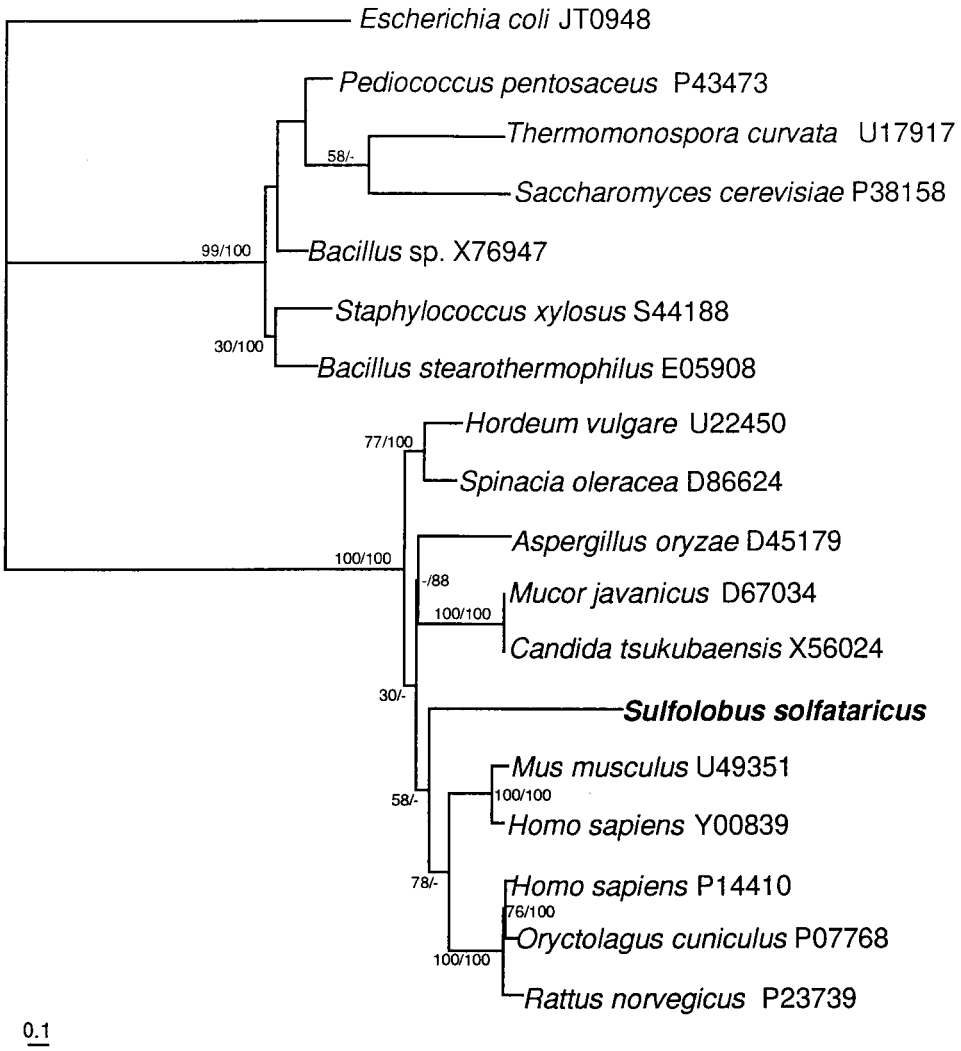

FIG. 6. Phylogenetic analysis of α-glucosidase and sucrase isomaltase sequences. A neighbor-joining distance tree is shown. Distances are indicated by the bar in the lower left corner, which represents 10 substitutions per 100 residues. Percent occurrence is given for nodes with values of >30%. Lower values are not shown or are indicated by a dash. Left-hand values are measures of distance; right-hand values are measures of parsimony. GenBank accession numbers are shown to the right of the names of the source organisms.

in the analysis, strain 98/2 from Yellowstone National Park and strain P2 (DSM 1617) from Italy. Genomic digests prepared with *Eco*RV (Fig. 5A) or *Hin*dIII (Fig. 5B) were then probed under stringent hybridization conditions with a 731-bp *Eco*RV-*Hin*dIII *malA* gene fragment encompassing nucleotides 714 to 1445 of the *malA* coding region (Fig. 1). Both strains of *S. solfataricus* exhibited strongly hybridizing bands of 2.9 kb following *Eco*RV digestion and 1.2 kb following *Hin*dIII digestion (Fig. 5, lanes 3 and 4), in agreement with the Southern blot results obtained previously with the 731-bp *Hin*dIII-*Eco*RV probe fragment derived from the initial *malA* PCR product. For *S. shibatae*, single weakly hybridizing bands of 0.65 kb following *Eco*RV digestion (Fig. 5A, lane 1) and 3.7 kb following *Hin*dIII digestion (Fig. 5B, lane 1) were also observed. No cross-hybridization was observed, however, between the *S. solfataricus malA* gene and *S. acidocaldarius* genomic DNA digests (Fig. 5, lanes 2).

Phylogenetic analysis of α-glucosidase sequences. Amino acid sequences of α-glucosidases and the related sucrase isomaltases were retrieved from the Swiss-Prot and EMBL/GenBank/DDBJ databases. A multiple sequence alignment of 6 bacterial and 11 eukaryotic sequences in addition to the *S. solfataricus* sequence was made. The region of the *S. solfataricus* α-glucosidase used for the alignment included 569 amino acid residues spanning positions 50 to 618. The *S. solfataricus* α-glucosidase is the only representative of the archaea, since no other archaeal α-glucosidases were found in the databases. A conserved stretch of amino acids located in the middle of the three fungal sequences was deleted to minimize sequence gaps in the alignment. The alignment of sequences then was analyzed by distance, parsimony, and maximum-likelihood methods. The *E. coli malZ* gene product was used as the outgroup. The sequences clustered into two groups typically of either eubacterial or eukaryotic affiliation by all three methods of analysis. Nearest-neighbor distance analysis and parsimony analysis indicate that the *S. solfataricus* α-glucosidase is most closely related to mammalian enzyme homologs (Fig. 6). Maximum-likelihood analysis gave similar results (data not shown).

Recombinant *S. solfataricus* α-glucosidase activity. To prove that *malA* encodes a hyperthermophilic α-glucosidase, the

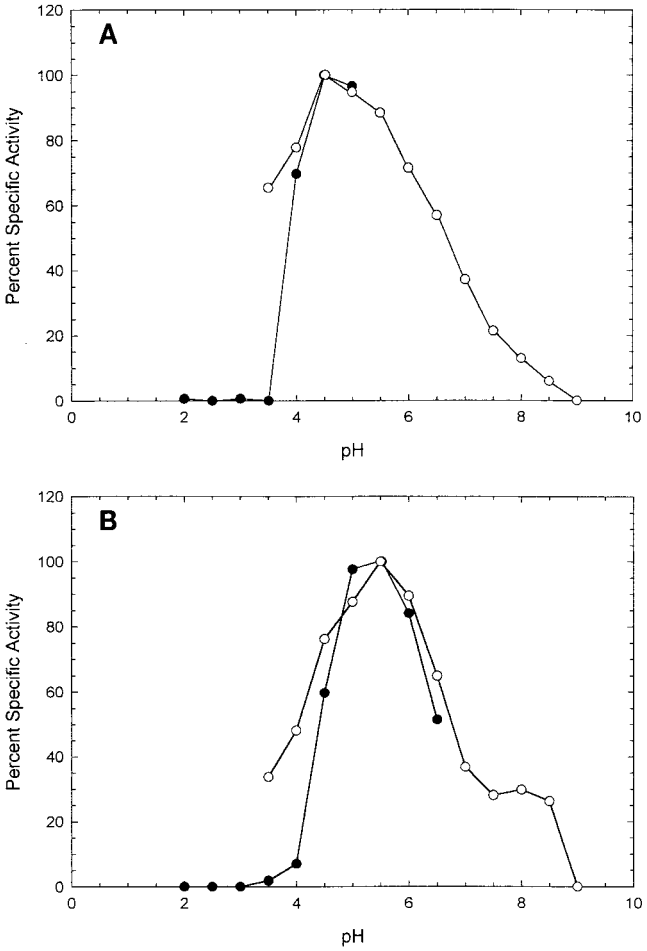

FIG. 7. pH optima for maltose and glycogen hydrolysis. (A) Maltose hydrolysis; (B) glycogen hydrolysis. Buffers were as follows: pH 2.0 to 5.0, 100 mM sodium acetate (closed circles); pH 3.5 to 9.0, 100 mM sodium phosphate (open circles).

malA gene was overexpressed in *E. coli* and the recombinant enzyme was purified and characterized. Purification of the recombinant enzyme to apparent homogeneity employed heat fractionation of clarified cell sonicates followed by anion-exchange fast protein liquid chromatography and gel filtration fast protein liquid chromatography as described previously (40). The recombinant *S. solfataricus* α-glucosidase exhibited significant recalcitrance to denaturation as indicated by its behavior during denaturing SDS-PAGE. Despite boiling in the presence of 2% (wt/vol) SDS for 10 min, the α-glucosidase failed to enter the separating gel and instead migrated in significant amounts (representing 45% of the total observed protein) in the stacking gel (data not shown). However, 95% of the natural enzyme treated in an identical manner was observed in the multimeric form (40), suggesting that the recombinant enzyme dissociates more readily under these conditions. Complete denaturation of the recombinant α-glucosidase required additional treatment with 6 M guanidine hydrochloride, resulting in exclusive formation of the 80-kDa monomer (data not shown). The purified recombinant enzyme hydrolyzed *p*-nitrophenyl-α-D-glucopyranoside with a K_m of 2.16 mM and a V_{max} of 3.08 μmol of *p*-nitrophenol/min at 85°C. It exhibited a pH optimum for maltose hydrolysis of 4.5 (Fig. 7A). In contrast to its apparent greater tendency to dissociate during SDS-PAGE, the recombinant α-glucosidase exhibited greater thermostability than the natural enzyme, with a half-life of 39 h at 85°C at a pH of 6.0.

α-Glucosidases of mammalian origin can be generally distinguished from those of higher plants and eubacteria by their affinities for glycogen as a substrate. Glycogen was hydrolyzed efficiently by the *S. solfataricus* enzyme. It exhibited a pH optimum for glycogen hydrolysis of 5.5 (Fig. 7B), a K_m of 64.9 mg/ml, and a V_{max} of 1.0 μmol of glucose/min at 85°C.

DISCUSSION

We report here the identification and characterization of the gene (*malA*) encoding the major soluble α-glucosidase (maltase) of *S. solfataricus*. This is the first report of an α-glucosidase sequence from the archaeal domain. The presence of an *S. solfataricus malA* homolog and corresponding α-glucosidase activity in *S. shibatae* suggests that these *Sulfolobus* species have similar pathways for the utilization of maltose and maltooligomers. Lack of a *malA* homolog or significant α-glucosidase activity in *S. acidocaldarius* may explain the inability of *S. acidocaldarius* to utilize maltose as a sole carbon and energy source. An α-glucosidase thus may be essential for utilization of maltose among certain members of the genus *Sulfolobus* and represents a distinguishing physiological feature for *Sulfolobus* species identification. Such metabolic divergence lends further support to the suggestion that the *Sulfolobus* genus be revised (8).

Maltose utilization by these *Sulfolobus* species necessitates mechanisms for assimilation of maltose or maltodextrins, and specific transport systems have been identified recently in *S. shibatae* (51). However, the purified *S. solfataricus* enzyme also uses glycogen as a substrate. *S. solfataricus* accumulates glycogen as the major intracellular storage polysaccharide (28); thus, glycogen utilization may require the *S. solfataricus* α-glucosidase. This is further supported by the observation that unlike maltose hydrolysis (40), glycogen hydrolysis by the *S. solfataricus* α-glucosidase exhibits a more neutral pH optimum approximating that of the intracellular environment of this organism (31). Perhaps a dual role for the α-glucosidase in the utilization of endogenous and exogenous polysaccharides can explain the apparent α-glucosidase activity observed in both *S. solfataricus* and *S. shibatae* during growth on glucose. Constitutive expression of *malA* may be necessary to balance catabolic and anabolic metabolic needs. Since eubacterial α-glucosidases lack glycogen-hydrolytic activity (33, 47, 48), the results presented here further distinguish archaeal α-glucosidases from those of eubacteria.

The large intergenic sequence located 5′ to *malA* is a distinguishing feature of the *malA* region. Northern blot analysis indicates that there is a lack of apparent transcripts encoded on either strand in the region covered by the dsDNA probe P2 (bp −651 to −152) produced during chemoheterotrophic growth on maltose. The entire intergenic region is also largely devoid of sequences encoding proteins; there is only one deduced sequence in excess of 39 residues (a protein of 88 residues) encoded in the region subjected to Northern analysis. However, this DNA sequence lacks a consensus promoter sequence and does not produce a detectable transcript during growth on maltose. Such noncoding regions are relatively rare in prokaryotic genomes, which are typically dense with genes. This is also true for the *S. solfataricus* P2 genome (42). It is therefore possible that the region 5′ to *malA* provides some additional function to the *S. solfataricus* genome. Genomic measurements of G+C mole percent compositions lend additional support to this idea. The G+C content of the *S. solfataricus* genome is 38

mol% (13, 15). However, the approximately 1-kb intergenic region lying 5′ to *malA* is distinctly lower in its G+C composition, with an average of 30 mol%, in contrast to the two flanking coding regions, which exhibit values of 38 mol%. It must therefore be assumed that intergenic regions such as this are rare in the *S. solfataricus* genome, as they would otherwise reduce global measurements of base composition.

Transcription of *malA* appears to utilize a consensus archaeal promoter motif. This sequence has been previously described as the box A motif TTTATA (11, 12). Gel shift analysis directly supports a role for the TATA box A region in the 5′ flanking region for *malA*. Complex formation was dependent upon the 3′-terminal 42 bp, of which the most 5′-terminal region comprises the TATA box A sequence. Additionally, primer extension analysis indicates that the point of transcription initiation is at the conserved guanine located within the so-called box B region. As this residue lies only 8 bp 5′ to the *malA* start codon, the mechanism employed for translation initiation of *malA* must operate within significant sequence constraints. Similar observations have been made for other archaeal genes, and as yet the mechanisms employed for translation initiation of these types of genes remain obscure.

Phylogenetic analysis of the α-glucosidase and sucrase isomaltase sequences by three methods (distance, parsimony, and maximum likelihood) yielded similar trees with nearly identical branching topologies. These methods place the *S. solfataricus* enzyme with those of eukaryotes, specifically mammals, rather than with eubacterial orthologs. Recent studies on the relatedness of archaea to eubacteria and eukaryotes have suggested that archaeal central metabolic enzymes exhibit greatest relatedness to those of eubacteria. The results presented here, however, indicate that at least some archaeal metabolic pathways, such as those associated with carbohydrate metabolism, may have an evolutionary origin more in common with those of certain eukaryotes.

ACKNOWLEDGMENTS

We thank D. Grogan for cultures.

This work was supported by NSF grants EPS-9255225 and MCB-9604000 and by the University of Nebraska Center for Biotechnology.

REFERENCES

1. **Allen, M. B.** 1959. Studies with *Cyanidium caldarium*, an anomalously pigmented chlorophyte. Arch. Mikrobiol. **32:**270–277.
2. **Birnboim, H. C., and J. Doly.** 1979. A rapid alkaline extraction procedure for screening recombinant plasmid DNA. Nucleic Acids Res. **7:**1513–1523.
3. **Blum, P., J. Bauernfiend, J. Ory, and J. Krska.** 1992. Physiological consequences of DnaK and DnaJ overproduction in *Escherichia coli*. J. Bacteriol. **174:**7436–7444.
4. **Bragger, J. M., R. M. Daniel, T. Coolbear, and H. W. Morgan.** 1989. Very stable enzymes from extremely thermophilic archaebacteria and eubacteria. Appl. Microbiol. Biotechnol. **31:**556–561.
5. **Brock, T. D., K. M. Brock, R. T. Belly, and R. L. Weiss.** 1972. *Sulfolobus*: a genus of sulfur oxidizing bacteria living at low pH and high temperature. Arch. Mikrobiol. **84:**54–68.
6. **Brown, T., and K. Mackey.** 1997. Analysis of RNA by Northern and slot blot hybridization, unit 4.9.1–4.9.13. *In* F. M. Ausubel, R. Brent, R. E. Kingston, D. D. Moore, J. G. Seidman, J. A. Smith, and K. Struhl (ed.), Current protocols in molecular biology. John Wiley and Sons, Inc., New York, N.Y.
7. **Buratowski, S., and L. A. Chodosh.** 1996. Mobility shift DNA-binding assay using gel electrophoresis, unit 12.2.1–12.2.7. *In* F. M. Ausubel, R. Brent, R. E. Kingston, D. D. Moore, J. G. Seidman, J. A. Smith, and K. Struhl (ed.), Current protocols in molecular biology. John Wiley and Sons, Inc., New York, N.Y.
8. **Burggraf, S., H. Huber, and K. O. Stetter.** 1997. Reclassification of the crenarchaeal orders and families in accordance with 16S rRNA sequence data. Int. J. Syst. Bacteriol. **47:**657–660.
9. **Chomczynski, P., and N. Sacchi.** 1987. Single-step method of RNA isolation by acid guanidinium thiocyanate-phenol-chloroform extraction. Anal. Biochem. **162:**156–159.
10. **Costantino, H. R., S. H. Brown, and R. M. Kelly.** 1990. Purification and characterization of an α-glucosidase from a hyperthermophilic archaebacterium, *Pyrococcus furiosus*, exhibiting a temperature optimum of 105 to 115°C. J. Bacteriol. **172:**3654–3660.
11. **Daalgard, J. Z., and R. A. Garret.** 1993. Archaeal hyperthermophile genes, p. 535–563. *In* M. Kates, D. J. Kushner, and A. T. Matheson (ed.), The biochemistry of Archaea. Elsevier Science Publishers, New York, N.Y.
12. **Dennis, P. P.** 1986. Molecular biology of archaebacteria. J. Bacteriol. **168:** 471–478.
13. **De Rosa, M., A. Gambacorta, and J. D. Bu'lock.** 1975. Extremely thermophilic acidophilic bacteria convergent with *Sulfolobus acidocaldarius*. J. Gen. Microbiol. **86:**156–164.
14. **Felsenstein, J.** 1989. PHYLIP—phylogeny inference package (version 3.2). Cladistics **5:**164–166.
15. **Grogan, D., P. Palm, and W. Zillig.** 1990. Isolate B12, which harbours a virus-like element, represents a new species of the archaebacterial genus *Sulfolobus*, *Sulfolobus shibatae*, sp. nov. Arch. Microbiol. **154:**594–599.
16. **Grogan, D. W.** 1989. Phenotypic characterization of the archaebacterial genus *Sulfolobus*: comparison of five wild-type strains. J. Bacteriol. **171:** 6710–6719.
17. **Grogan, D. W.** 1991. Evidence that β-galactosidase of *Sulfolobus solfataricus* is only one of several activities of a thermostable β-D-glycosidase. Appl. Environ. Microbiol. **57:**1644–1649.
18. **Hanahan, D.** 1983. Studies on transformation of *Escherichia coli* with plasmids. J. Mol. Biol. **166:**557.
19. **Haseltine, C., M. Rolfsmeier, and P. Blum.** 1996. The glucose effect and regulation of α-amylase synthesis in the hyperthermophilic archaeon *Sulfolobus solfataricus*. J. Bacteriol. **178:**945–950.
20. **Hermans, M. M. P., M. A. Kroos, J. van Beeumer, B. A. Oostra, and A. J. J. Reuser.** 1991. Human lysosomal α-glucosidase. J. Biol. Chem. **266:**13507–13512.
21. **Hers, H. G.** 1963. α-Glucosidase deficiency in generalized glycogen-storage disease (Pompe's disease). Biochem. J. **86:**11–16.
22. **Hochstein, L. I., and H. Stan-Lotter.** 1992. Purification and properties of an ATPase from *Sulfdobus solfataricus*. Arch. Biochem. Biophys. **295:**153–160.
23. **Huber, G., and K. O. Stetter.** 1991. *Sulfolobus metallicus*, sp. nov., a novel strictly chemolithoautotrophic thermophilic archaeal species of metal-mobilizers. Syst. Appl. Microbiol. **14:**372–378.
24. **Hudepohl, U., W.-D. Reiter, and W. Zillig.** 1990. *In vitro* transcription of two rRNA genes of the archaebacterium *Sulfolobus sp.* B12 indicates a factor requirement for specific initiation. Proc. Natl. Acad. Sci. USA **87:**5851–5855.
25. **Kandler, O., and K. O. Stetter.** 1981. Evidence for autotrophic CO_2 assimilation in *Sulfolobus brierleyi* via a reductive carboxylic acid pathway. Zentralbl. Bakteriol. Hyg. Abt. 1 Orig. C **2:**111–121.
26. **Kelly, C. T., and W. M. Fogarty.** 1983. Microbial α-glucosidases. Process Biochem. **18:**6–12.
27. **Kondo, S., A. Yamagishi, and T. Oshima.** 1991. Positive selection for uracil auxotrophs of the sulfur-dependent thermophilic archaebacterium *Sulfolobus acidocaldarius* by use of 5-fluoroorotic acid. J. Bacteriol. **173:**7698–7700.
28. **Konig, H., R. Skorko, W. Zillig, and W.-D. Reiter.** 1982. Glycogen in thermoacidophilic archaebacteria of the genera *Sulfolobus*, *Thermoproteus*, *Desulfurococcus* and *Thermococcus*. Arch. Microbiol. **132:**297–303.
29. **Krska, J., T. Elthon, and P. Blum.** 1993. Monoclonal antibody recognition and function of a DnaK (HSP70) epitope found in gram-negative bacteria. J. Bacteriol. **175:**6433–6440.
30. **Kurosawa, N., and Y. H. Itoh.** 1993. Nucleotide sequence of the 16S rRNA gene from thermoacidophilic archaea *Sulfolobus acidocaldarius* ATCC33909. Nucleic Acids Res. **21:**357.
31. **Lübben, M., and G. Schäfer.** 1989. Chemiosmotic energy conversion of the archaebacterial thermoacidophile *Sulfolobus acidocaldarius*: oxidative phosphorylation and the presence of an F_0-related *N,N′*-dicyclohexylcarbodiimide-binding proteolipid. J. Bacteriol. **171:**6106–6116.
32. **Matsudaira, P.** 1990. Limited N-terminal sequence analysis. Methods Enzymol. **182:**602–613.
33. **McWethy, S. J., and P. A. Hartman.** 1979. Extracellular maltase of *Bacillus brevis*. Appl. Environ. Microbiol. **37:**1096–1102.
34. **Nucci, R., M. Moracci, C. Vaccaro, N. Vespa, and M. Rossi.** 1993. Exoglucosidase activity and substrate specificity of the β-glycosidase isolated from the extreme thermophile *S. solfataricus*. Biotechnol. Appl. Biochem. **17:** 239–250.
35. **Olsen, G. J., N. R. Pace, M. Nuell, B. P. Kaine, R. Gupta, and C. R. Woese.** 1985. Sequence of the 16S rRNA gene from the thermoacidophilic archaebacterium *Solfataricus solfataricus* and its evolutionary implications. J. Mol. Evol. **22:**301–307.
36. **Qureshi, S. A., P. Baumann, T. Rowlands, B. Khoo, and S. P. Jackson.** 1995. Cloning and functional analysis of the TATA binding protein from *Solfataricus shibatae*. Nucleic Acids Res. **23:**1775–1781.
37. **Reiter, W.-D., P. Palm, and W. Zillig.** 1988. Analysis of transcription in the archaebacterium *Sulfolobus* indicates that archaebacterial promoters are homologous to eukaryotic pol II promoters. Nucleic Acids Res. **16:**1–19.
38. **Rockabrand, D., T. Arthur, G. Korinek, K. Lievers, and P. Blum.** 1995. An essential role for the *Escherichia coli* DnaK protein in starvation-induced

thermotolerance, H_2O_2 resistance, and reductive division. J. Bacteriol. **177:** 3695–3703.
39. **Rockabrand, D., and P. Blum.** 1995. Multicopy plasmid suppression of stationary phase chaperone toxicity in *Escherichia coli* by phosphogluconate dehydratase and the N-terminus of DnaK. Mol. Gen. Genet. **249:**498–506.
40. **Rolfsmeier, M., and P. Blum.** 1995. Purification and characterization of a maltase from the extremely thermophilic crenarchaeote *Solfolobus solfataricus*. J. Bacteriol. **177:**482–485.
41. **Sambrook, J., E. F. Fritsch, and T. Maniatis.** 1989. Molecular cloning: a laboratory manual, 2nd ed. Cold Spring Harbor Laboratory Press, Cold Spring Harbor, N.Y.
42. **Sensen, C. W., H. P. Klenk, R. K. Singh, G. Allard, C. C.-Y. Chan, Q. Y. Liu, S. L. Penny, F. Young, M. E. Schenk, T. Gaasterland, W. F. Doolittle, M. A. Ragan, and R. L. Charlebois.** 1996. Organizational characteristics and information content of an archaeal genome: 156 kb of sequence from *S. solfataricus* P2. Mol. Microbiol. **5:**1687–1693.
43. **Strimmer, K., and A. von Haeseler.** 1996. Quartet puzzling: a quartet maximum likelihood method for reconstructing tree topologies. Mol. Biol. Evol. **13:**964–969.
44. **Takayanagi, S., H. Kawaski, K. Sugimori, T. Yamada, A. Sugai, T. Ito, K. Yamasato, and M. Shioda.** 1996. *Sulfolobus hakonensis* sp. nov., a novel species of acidothermophilic archaeon. Int. J. Syst. Bacteriol. **46:**377–382.
45. **Thompson, J. D., D. G. Higgins, and T. J. Gibson.** 1994. CLUSTAL W: improving the sensitivity of progressive multiple sequence alignment through sequence weighting, positions-specific gap penalties and weight matrix choice. Nucleic Acids Res. **22:**4673–4680.
46. **Triezenberg, S. J.** 1992. Primer extension, unit 4.8.1–4.8.4. *In* F. M. Ausubel, R. Brent, R. E. Kingston, D. D. Moore, J. G. Seidman, J. A. Smith, and K. Struhl (ed.), Current protocols in molecular biology. John Wiley and Sons, Inc., New York, N.Y.
47. **Urlab, H., and G. Wober.** 1978. α-Glucosidase, a membrane-bound enzyme of α-glucan metabolism in *Bacillus amyloliquefaciens*. Biochim. Biophys. Acta **522:**161–173.
48. **Wang, L. H., and P. A. Hartman.** 1976. Purification and some properties of an extracellular maltase from *Bacillus subtilis*. Appl. Environ. Microbiol. **31:** 108–118.
49. **Woese, C., O. Kandler, and M. L. Wheelis.** 1990. Towards a natural system of organisms: proposal for the domains archaea, bacteria and eucarya. Proc. Natl. Acad. Sci. USA **87:**4576–4579.
50. **Wood, A. P., D. P. Kelly, and P. R. Norris.** 1987. Autotrophic growth of four *Sulfolobus* strains on tetrathionate and the effect of organic nutrients. Arch. Microbiol. **146:**382–389.
51. **Yallop, C. A., and B. M. Charalambous.** 1996. Nutrient utilization and transport in the thermoacidophilic archaeon *Sulfolobus shibatae*. Microbiology **142:**3373–3380.
52. **Yeats, S., P. McWilliams, and W. Zillig.** 1982. A plasmid in the archaebacterium *Sulfolobus acidocaldarius*. EMBO J. **1:**1035–1038.
53. **Zillig, W.** 1993. Confusion in the assignments of *Sulfolobus* sequences to *Sulfolobus* species. Nucleic Acids Res. **21:**5273.
54. **Zillig, W., A. Lketzin, C. Schleper, I. Holz, D. Janekovic, J. Hain, M. Lanzendorder, and J. K. Kristjansson.** 1994. Screening for *Sulfolobales*, their plasmids and their viruses in Icelandic solfataras. Syst. Appl. Microbiol. **16:** 609–628.